Influence of the interaction between quasiparticles on parametric resonance in Bose-Einstein quasicondensates

Maciej Pylak and Paweł Zin*
National Centre for Nuclear Research, ul. Hoża 69, 00-681 Warsaw, Poland

(Received 23 April 2018; published 2 October 2018)

We perform a simulation of the experiment [J. C. Jaskula *et al.*, Phys. Rev. Lett. **109**, 220401 (2012)] where the temporal modification of the effective one-dimensional interaction constant was used to create pairs of atoms with opposite velocities. The simulations clearly demonstrate the huge impact of the interaction between quasiparticles due to finite temperature on the pair production process, explaining the relatively small atomic pair production and the absence of number squeezing in the experiment.

DOI: 10.1103/PhysRevA.98.043603

I. INTRODUCTION

The generation of nonclassical states in atomic ensembles is a rapidly developing direction in trapped ion and cold neutral atomic physics [1]. Such states can be used to increase the sensitivity of precision measurements beyond the standard classical limit [2]. A hundred times decrease of measurement noise beyond the classical limit was recently reported in cold thermal atoms [3]. One of the possible states that is particle entangled, and can be used to increase the sensitivity of precision measurements, is a so-called twin-Fock state $|n, n\rangle$ [4,5]. Such a state can be created in experiments generating atomic pairs with well-defined momenta in quasi-one-dimensional (1D) systems. This was done by modulation of the effective one-dimensional atomic interaction parameter [6], or a modulation instability present in a one-dimensional lattice [7], or else by the decay of an excited state [8]. The theoretical analysis for these situations was performed using the Bogoliubov approximation [9–11]. In this case, the Hamiltonian is quadratic in field operators. It has the term responsible for the creation of atomic pairs but neglects higher-order terms in the field operators, which describe the interaction between quasiparticles. As the process of pair creation starts, the atoms, according to the Bogoliubov description, are created in pairs with well-defined momenta. Therefore, one expects the violation of Cauchy-Schwartz inequality, which is a clear signature of entanglement [12]. Such a violation was observed in two of the above-mentioned experiments [7,8]. However, it was not seen in the experiment described in Ref. [6]. This suggests that the interaction between quasiparticles, neglected in the Bogoliubov approximation, can influence pair production. We performed such an analysis for a three-dimensional homogeneous system in the case of pair creation caused by temporal modulation of the interaction parameter [13]. There, it was found that indeed the interaction between quasiparticles may drastically change the pair creation process. The parametric process is described by a single parameter δ responsible for the strength of the amplification, while the interaction between quasiparticles is described by a quasiparticle decay constant γ. When $\delta > \gamma$, the pair production process is roughly given by $\exp[2(\delta - \gamma)t]$, leading always to a huge number of pairs produced if t is large enough. On the other hand, if $\gamma > \delta$, the number of pairs produced tends to a constant for $t \to \infty$. Additionally, we have found that, depending on the parameters of the system, the Cauchy-Schwartz inequality may or may not be violated.

In the present paper we perform a numerical simulation of the experiment [6] using the classical field method [14]. The obtained results agree with the experimental measurements showing a relatively small pair production and the lack of a Cauchy-Schwartz equality violation. To get a deeper understanding of the obtained results we perform a numerical simulation of the homogeneous analog of the experimental system. There, we additionally perform an analysis based on the Bogoliubov method. For temperatures much smaller than in the experiment, the classical field method results agree with the Bogoliubov method predictions, showing a huge number of pairs produced. But when the temperature tends to the experimental value, the production process practically stops with a relatively small number of atomic pairs produced, which is in agreement with the experiment. To check if the condition derived in Ref. [13] applies to the one-dimensional case, we numerically compute γ as well as the number of atomic pairs produced as a function of temperature. We find that the number of pairs produced tends to a constant if γ is approximately equal to δ, which validates the suggested condition.

The paper is organized as follows. In Sec. II we describe the system of interest. There, we introduce the classical field method as an approximate method of description. In Sec. III, using the Bogoliubov approximation to the classical field method, we construct an initial thermal state of the system. In Sec. IV we simulate the pair creation process for both homogeneous and inhomogeneous systems. We conclude in Sec. V.

II. THEORETICAL MODEL

We consider the system described in Ref. [6]. There, we have $N = 10^5$ helium atoms of temperature

*Pawel.zin@ncbj.gov.pl

 ©2018 American Physical Society

$T = 200$ nK put in a harmonic trapping potential $V(\mathbf{r}) = \frac{1}{2}m[\omega_r^2(y^2+z^2)+\omega_x^2 x^2]$ with $\omega_r = 1500 \times 2\pi$ Hz and $\omega_x = 7 \times 2\pi$ Hz. The atoms interact via a contact potential characterized by the parameter $g_{3d} = \frac{4\pi\hbar^2 a}{m}$, where $a = 7.51$ nm is the metastable helium scattering length. In the experiment the laser intensity oscillates in time, which causes oscillations of the trapping frequencies. When oscillation ends, the trapping potential is turned off, the atoms freely expand, and finally fall on the detector. The measurement of a time of arrival and a position of the atom detected allows for a reconstruction of the atomic velocity correlation functions.

Let us now introduce the theoretical model of the above experimental scenario. Assume first we deal with the system which is trapped in the y and z directions and is uniform in x. Such a system was analyzed in Ref. [15]. There, the author finds that low-energy excitations are given by the one-dimensional model with the effective interaction constant given by

$$g = g_{3d}\frac{\int dydz\, n_{3d}^2(y,z)}{[\int dydz\, n_{3d}(y,z)]^2}, \tag{1}$$

where $n_{3d}(y,z)$ is the solution of the stationary Gross-Pitaevskii equation

$$\left(-\frac{\hbar^2}{2m}\Delta + V_\perp + g_{3d}n_{3d}(y,z) - \mu_{3d}\right)\sqrt{n_{3d}(y,z)} = 0,$$

with $V_\perp(y,z) = \frac{1}{2}m\omega_r^2(y^2+z^2)$. The fact that the low-energy excitations are given by a one-dimensional model seems intuitive. It seems impossible to excite the system in the transverse direction (y or z) as long as the energy of excitation is much smaller than the characteristic excitation energy in the transverse direction roughly equal to $\hbar\omega_r$. Thus the excited modes of the system have the form $\varphi_0(y,z)\exp(ikx)$, where

$$\varphi_0(y,z) = \sqrt{\frac{n_{3d}(y,z)}{\int dydz\, n_{3d}(y,z)}}.$$

As the excitations of the system are now limited to the above class, the three-dimensional field operator $\hat{\psi}(\mathbf{r})$ becomes equal to $\varphi_0(y,z)\hat{\psi}(x)$. where $\hat{\psi}(x)$ is the one-dimensional field operator. Then, the contact interaction equal to

$$\begin{aligned} &g_{3d}\hat{\psi}^\dagger(\mathbf{r})\hat{\psi}^\dagger(\mathbf{r})\hat{\psi}(\mathbf{r})\hat{\psi}(\mathbf{r}) \\ &\quad = g_{3d}|\varphi_0(y,z)|^4\hat{\psi}^\dagger(x)\hat{\psi}^\dagger(x)\hat{\psi}(x)\hat{\psi}(x) \end{aligned}$$

can be integrated over the y and z coordinates. It results in a one-dimensional interaction with the constant given by Eq. (1). The above can be generalized to the nonuniform system with $g(x)$ equal to

$$g(x) = g_{3d}\frac{\int dydz\, n_{3d}^2(\mathbf{r})}{[\int dydz\, n_{3d}(\mathbf{r})]^2}, \tag{2}$$

where $n_{3d}(\mathbf{r})$ is given by the solution of

$$\left(-\frac{\hbar^2}{2m}\Delta + V(\mathbf{r}) + g_{3d}n_{3d}(\mathbf{r}) - \mu_{3d}\right)\sqrt{n_{3d}(\mathbf{r})} = 0, \tag{3}$$

with the normalization condition $\int d\mathbf{r}\, n_{3d}(\mathbf{r}) = N$. The above is valid as long as we consider excitations with an energy much smaller than the characteristic excitation energy in the transverse direction [16].

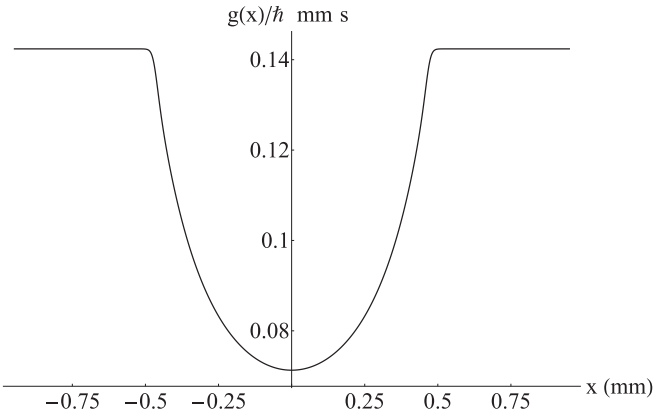

FIG. 1. Effective 1D-interaction parameter.

The function $g(x)$ obtained using Eq. (2) is plotted in Fig. 1. One can clearly see the position dependence of the interaction parameter. As we shall see later, oscillation of the trapping frequencies causes the effective interaction constant to be time dependent, $g(x,t)$. We further approximate the description of the system by relying on the classical field method [14]. This approximation is allowable if the system is weakly interacting, i.e., if $\gamma \ll 1$, where

$$\gamma = \frac{mg}{\hbar^2 n}, \tag{4}$$

and n being the one-dimensional particle density. For our system we can approximate $n(x) \simeq \int dydz\, n_{3d}(\mathbf{r})$, which gives $n(0) \simeq 1.8 \times 10^8$ atoms/m and $\gamma \simeq \frac{mg(0)}{\hbar^2 n(0)} \simeq 2.5 \times 10^{-5}$ which justifies the use of the classical field approximation. In this method we substitute creation and annihilation operators of highly populated modes with c-numbers $\hat{a}_\nu \to \alpha_\nu$. To perform this approximation we approximate the continuous space by the finite lattice. The Hamiltonian of the system takes the form

$$\begin{aligned} \hat{H} = &\sum_x \Delta x\, \hat{\Psi}^\dagger(x)\left(-\frac{\hbar^2}{2m}\triangle_d + V(x)\right)\hat{\Psi}(x) \\ &+ \sum_x \Delta x\frac{g(x,t)}{2}\hat{\Psi}^\dagger(x)\hat{\Psi}^\dagger(x)\hat{\Psi}(x)\hat{\Psi}(x), \end{aligned} \tag{5}$$

where the sum is over discrete points $x = \frac{j}{M}L$, $j = 1,\ldots,M$, with L being the length of the system and $\Delta x = \frac{L}{M}$. Additionally, $\triangle_d$ is a finite matrix approximation of the one-dimensional Laplacian that we shall specify later on. We consider the harmonic external potential $V(x) = \frac{1}{2}m\omega^2 x^2$ and, as mentioned above, the time- and position-dependent interaction parameter $g(x,t)$. The commutation relation takes the form $[\Psi(x), \Psi^\dagger(y)] = \frac{\delta_{x,y}}{\Delta x}$ and leads to the Heisenberg equation of motion,

$$\begin{aligned} i\hbar\partial_t\hat{\Psi}(x,t) = &\left(-\frac{\hbar^2}{2m}\triangle_d + V(x)\right)\hat{\Psi}(x,t) \\ &+ g(x,t)\hat{\Psi}^\dagger(x,t)\hat{\Psi}(x,t)\hat{\Psi}(x,t). \end{aligned} \tag{6}$$

In the classical field approximation the field operator $\hat{\Psi}(x,t)$ turns into the classical field $\psi(x,t)$. Then (6) becomes the

well-known Gross-Pitaevskii (GP) equation

$$i\hbar\partial_t\psi(x,t) = \left(-\frac{\hbar^2}{2m}\triangle_d + V(x)\right)\psi(x,t) + g(x,t)|\psi(x,t)|^2\psi(x,t). \quad (7)$$

We now deal with realizations of the classical field $\psi(x,t)$. For each time t the field $\psi(x,t)$ now becomes a point in the space of one-dimensional functions. The quantum state is now represented by a probability distribution $P[\psi(x,t)]$ defined on this functional space. The quantum averages are now substituted by averages over this probability distribution. Initially, the system is in thermal equilibrium. Since it is isolated, one should use the microcanonical ensemble to describe the state of the system, thus $P[\psi(x,0)]$ is the microcanonical ensemble probability distribution. Having $P[\psi(x,0)]$, we can calculate the mean value of any observables in $t = 0$. For $t > 0$ we proceed in the following way. We draw a single random $\psi(x,0)$ from $P[\psi(x,0)]$ which gives us a single realization of $\psi(x,0)$. Then, each realization is evolved using (7) to the final time. The observables are then calculated as the averages over the realizations. One of the parameters of control in the microcanonical ensemble is the energy of the system. However, in the experiment the temperature is the measured parameter. Thus we need to generate single realizations $\psi(x,0)$ for a given temperature. This seems to be a complicated task and we have chosen another, approximate way of obtaining the initial state with the desired temperature which we describe in the following section.

III. TEMPERATURE DIAGNOSTICS AND INITIAL-STATE PREPARATION

For low enough temperatures the weakly interacting one-dimensional gas enters the quasicondensate regime, where it is described as a system of weakly interacting Bogoliubov quasiparticles [17]. There, the classical field (in the quantum description, the field operator) is represented as

$$\psi(x,0) = \sqrt{n(x)+\delta n(x)}e^{i\phi(x)}, \quad (8)$$

where

$$\delta n(x) = \sqrt{n(x)}\sum_\nu f_\nu^-(x)\alpha_\nu + \text{c.c.}, \quad (9)$$

$$\phi(x) = \frac{1}{\sqrt{4n(x)}}\sum_\nu -if_\nu^+(x)\alpha_\nu + \text{c.c.} \quad (10)$$

In the above, α_ν, $\hbar\omega_\nu$, and $f_\nu^\pm$ are mode amplitudes, energies, and mode functions, respectively, obtained via the solution of Bogoliubov–de Gennes equations

$$[H_0(x) - \hbar\omega_\nu]u_\nu(x) - g(x)n(x)v_\nu(x) = 0, \quad (11)$$

$$[H_0(x) + \hbar\omega_\nu]v_\nu(x) - g(x)n(x)u_\nu(x) = 0, \quad (12)$$

where $f_\nu^\pm = u_\nu \pm v_\nu$ are normalized by the condition

$$\sum_x \Delta x\left[f_\nu^+(x)\right]^* f_{\nu'}^-(x) = \delta_{\nu,\nu'}. \quad (13)$$

Here, $n(x)$ is given by the solution of the stationary GP equation

$$H_0(x)\sqrt{n(x)} = 0, \quad (14)$$

with the normalization condition $\sum_x \Delta x\, n(x) = N$, where

$$H_0 = -\frac{\hbar^2}{2m}\triangle_d + V(x) + 2g(x)n(x) - \mu.$$

Neglecting the weak interaction between quasiparticles, the Hamiltonian of the system is $H \simeq \sum_\nu \hbar\omega_\nu|\alpha_\nu|^2$. The above description motivates us to approximate the probability distribution $P[\psi(x,0)]$ by the one corresponding to the canonical ensemble of noninteracting quasiparticles, that is, $P[\psi(x,0)] = \prod_\nu P(\alpha_\nu)$, where

$$P(\alpha_\nu) = \frac{\hbar\omega_\nu}{\pi k_B T_{\text{in}}}\exp\left(-\frac{\hbar\omega_\nu}{k_B T_{\text{in}}}|\alpha_\nu|^2\right), \quad (15)$$

where T_{in} denotes the initial temperature.

We now specify the finite matrix approximation to the one-dimensional Laplacian $\triangle_d$ by taking the one given by the discrete Fourier transform

$$-\triangle_d(x,x_k) = \frac{1}{M}\sum_k k^2 e^{ik(x-x_k)} = \left(\frac{2\pi}{L}\right)^2\left(\frac{(-1)^x}{2\sin^2\left(\frac{\pi}{M}x\right)}(1-\delta_x) + \delta_x C\right),$$

where $k = 2\pi\frac{m}{M}$, $x = \frac{x-x_k}{\Delta x}$, $-\frac{M}{2}+1 \leqslant m \leqslant \frac{M}{2}$, and $C = \frac{1}{M}\sum_{m=-M/2+1}^{M/2} m^2 = \frac{1}{12}(M^2+2)$. By doing so we implicitly assume a periodic boundary condition. Having specified $\triangle_d$ and knowing $g(x)$ we solve the one-dimensional GP equation (14), obtaining a Thomas-Fermi radius equal to $R = 0.46$ mm, a chemical potential $\frac{\mu}{\hbar} = 2.05\times 2\pi$ kHz, and the maximal density of the system equal to $n \simeq 1.8\times 10^8$ atoms/m. Before a further analysis of the nonuniform system, let us first analyze its homogeneous analog.

A. Homogeneous system

The parameters of the homogeneous system were chosen in the following way. We take the interaction parameter $g = g(0)$ and the mean density equal to the maximal density of the trapped system so that the chemical potentials of both uniform and nonuniform systems are the same. The box size is chosen to be equal to $L = 2R = 0.92$ mm with $M = 1024$ points. In the homogeneous case the solution of the Bogoliubov–de Gennes equations takes the analytical form [17]

$$f_k^\pm(x) = \frac{1}{\sqrt{L}}\left(\frac{\hbar\omega_k}{E_k}\right)^{\pm 1/2}e^{ikx} = f_k^\pm e^{ikx}, \quad (16)$$

where

$$\hbar\omega_k = \sqrt{E_k(E_k+2ng)} \quad (17)$$

and $E_k = \frac{\hbar^2k^2}{2m}$. We additionally calculate the density fluctuations equal to

$$\frac{\langle\delta n^2\rangle}{n^2} = \frac{2}{n}\sum_k\left(f_k^-\right)^2\langle|\alpha_k|^2\rangle = \frac{k_BT}{n\pi}\int dk\frac{1}{E_k+2ng} = \frac{k_BT}{ng}\sqrt{\gamma},$$

where γ is given by Eq. (4). To obtain the above, we used Eqs. (9), (16), (17), and (15). For the parameters given above and $T_{\rm in} = 200$ nK we obtain $\sqrt{\langle \delta n^2 \rangle}/n \simeq 0.1$. The fact that it is significantly smaller than unity justifies the use of the Bogoliubov method.

The single realization of the initial state $\psi(x,0)$ is constructed using Eqs. (9), (10), and (8) upon drawing α_ν randomly from the distribution (15) with chosen $T_{\rm in}$. Still, this is not the end of the construction. However, as we have written above, the distribution (15) neglects the interaction between quasiparticles. To get the initial state we proceed in the following way. We evolve the just constructed state using GP equation (7) with $g(x,t) = g(x)$ and $V(x) = 0$ for a sufficiently long time. After some time, due to the interaction between quasiparticles present in the GP equation, the system thermalizes and reaches its equilibrium state. In fact, we do not know the temperature of this state. We find its approximate value T using a procedure described below based on the Bogoliubov method. If $T \simeq T_{\rm in}$, then the influence of interaction between the quasiparticles on the temperature is negligible and it is justified to state that the temperature of the prepared state is equal to $T_{\rm in}$.

The approximate procedure to extract the temperature uses the decomposition

$$\delta n(x,t) = \sqrt{n(x)} \sum_k f_k^-(j)(x)\alpha_k(t) + \text{c.c.}, \tag{18}$$

$$\phi(x,t) = \frac{1}{\sqrt{4n(x)}} \sum_k -i f_k^+(x)\alpha_k(t) + \text{c.c.}, \tag{19}$$

where $|\alpha_k(t)|$ are time dependent due to the interaction between the quasiparticles omitted in the Bogoliubov approximation. Using the orthogonality condition (13) together with the above equations, we obtain

$$\alpha_k(t) = \sum_x \Delta x \frac{1}{\sqrt{L}} e^{-ikx} \left(f_k^+ \frac{\delta n(x,t)}{2\sqrt{n}} + i f_k^- \sqrt{n}\phi(x,t) \right), \tag{20}$$

where we used the fact that $f_k^\pm$ are real. In every single realization having $\psi(x,t)$, we find $\delta n(x,t)$ and $\phi(x,t)$ and upon inserting it into (20) we obtain all $\alpha_k(t)$. This enables us to find the average over many realizations $\langle |\alpha_k|^2 \rangle = \frac{1}{N_r} \sum_{r=1}^{N_r} |\alpha_{k,r}|^2$, where N_r denotes the number of realizations. We assume the distribution of α_k to be given by the formula (15) with $T_{\rm in}$ changed into the k-dependent final temperature T_k. We derive the equipartition formula $\langle |\alpha_k|^2 \rangle = \int d^2\alpha_k |\alpha_k|^2 P(\alpha_k) = \frac{k_B T_k}{\hbar \omega_k}$ which connects numerically calculated averages $\langle |\alpha_k|^2 \rangle$ with the final temperature T_k.In Fig. 2 we plot the ratio $T_k/T_{\rm in}$ as the function of n where $k = \frac{2\pi n}{L}$ for $T_{\rm in} = 50$ and 200 nK. We clearly see that T_k fluctuates around the value being very close to the initial temperature $T_{\rm in}$. That shows that the temperature of the thermalized state is equal to $T_{\rm in}$.

B. Inhomogeneous system

As in the homogeneous case, here we would like to use the Bogoliubov method to prepare the initial thermal state with the given temperature $T_{\rm in}$. However, the Bogoliubov method described above is a correct approximation in the bulk region of the system where $\delta n/n \ll 1$. At the edges of the system

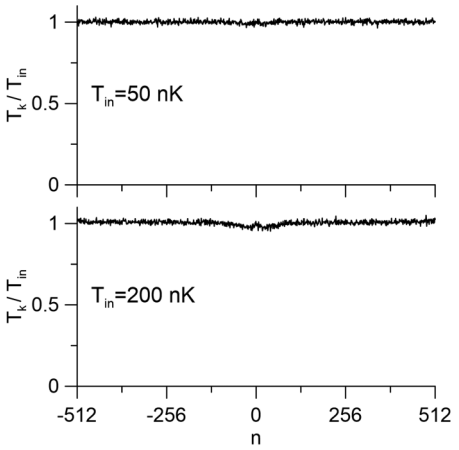

FIG. 2. The ratio $T_k/T_{\rm in}$ as the function of n where $k = 2\pi n/L$ for $T_{\rm in} = 50$ and 200 nK.

where n is negligible and a thermal cloud dominates, the condition $\delta n/n \ll 1$ is no longer satisfied and the Bogoliubov method cannot be used. Still, we need to construct a classical field $\psi(x,0)$ in that region. Below, we describe the approximate method to do that.

We divide our system into three parts: the bulk region $|x| < x_0$ ($x_0 < R$), where the condition $\delta n/n \ll 1$ is satisfied and where we use the Bogoliubov description. The region outside the quasicondensate $|x| > R$, where n is practically equal to zero. As we checked numerically in that region, $v_\nu(x) \simeq 0$ and the Bogoliubov equations (12) take an approximate form

$$\left(-\frac{\hbar^2}{2m} \triangle_d + V(x) \right) u_\nu(x) = (\mu + \epsilon_\nu) u_\nu(x).$$

The above equation is not a surprise since in that region we in fact neglect the nonlinear term $g|\psi|^2\psi$ in the GP equation (7), ending up with a noninteracting gas. Then, the classical field simply equals to

$$\psi_\mp(x,0) = e^{i\phi_\mp} \sum_\nu u_\nu(x)\alpha_\nu, \tag{21}$$

where $\psi_\mp$ denotes the field in the $x < -R$ and $x > R$ regions. Above we have also introduced phases $\phi_\mp$ for a reason which shall become clear later. The last region is $x_0 < |x| < R$, where $n(x) \neq 0$ but the condition $\delta n/n \ll 1$ is not satisfied. In that region we take

$$\psi_\mp(x) = A_\mp(x) e^{i\phi_\mp} [\sqrt{n(x)} + \delta\psi(x)], \tag{22}$$

where

$$\delta\psi = \sum_\nu \left(u_\nu \alpha_\nu - v_\nu \alpha_\nu^* \right). \tag{23}$$

We introduce the $A_\mp(x)e^{i\phi_\mp}$ factor where we take $A_\mp$ as a real function to match the continuity conditions at $|x| = x_0$ which take the form

$$A_\mp(\mp x_0) e^{i\phi_\mp} [\sqrt{n(\mp x_0)} + \delta\psi(\mp x_0)] = \sqrt{n(\mp x_0) + \delta n(\mp x_0)} e^{i\phi(\mp x_0)}. \tag{24}$$

Using Eq. (23) and the fact that in the region $|x| > R$, $v_\nu(x) \simeq 0$, we rewrite Eq. (21) as

$$\psi_\mp(x,0) = e^{i\phi_\mp}\delta\psi(x,0), \tag{25}$$

where $\phi_\mp$ is given by the numerical solution of Eq. (24). Then, the continuity condition at $x = \mp R$, where $n(\pm R) = 0$, implies $A_\mp(\mp R) = 1$. To fully define the classical field we need to specify the function $A_\mp(x)$ between $|x| = x_0$ and $|x| = R$. We make the simplest choice of linear function,

$$A_\mp(x) = A_\mp(\mp x_0)\frac{R-|x|}{R-x_0} + \frac{|x|-x_0}{R-x_0},$$

where $A_\mp(\mp x_0)$ is given by the numerical solution of Eq. (24). The single realization of the classical field ψ consists of drawing α_ν from the distribution (15) and inserting it into Eqs. (9), (10), and (8) to get the bulk region part and in Eqs. (22), (23), and (25) to get the tails of ψ.

In the numerical code for the inhomogeneous case we took $M = 1024$ points with the box size $L = 1.9$ mm. Having $g(x)$ and the $\triangle_d$ operator we numerically diagonalize the Bogoliubov–de Gennes equations (12). In the one-dimensional case, $f_\nu^\pm$ can be chosen to be real. Then, using the above scheme, we construct the initial state for two temperatures $T_{\rm in} = 50$ and 200 nK. We take $x_0 = 0.95R$ to be as close the border of the $n(x)$ as possible, at the same time satisfying $\delta n/n \ll 1$. As in the homogeneous case, we evolve such a constructed state according to (7) by taking $g(x,t) = g(x)$ and allowing the system to thermalize to a final temperature. Due to the fact that the Bogoliubov method is valid only in the bulk region, the procedure of extracting temperature from a given state is more complicated than in the homogeneous case. The bulk region seems to be the most convenient one to be used in extracting the temperature. We define

$$A_\nu = \frac{1}{2}\sum_x \Delta x\, f_\nu^+(x)\frac{\delta n(x,t)}{\sqrt{n(x)}}. \tag{26}$$

From (18) we obtain that

$$A_\nu = \sum_{\nu'} c_{\nu\nu'}\,\mathrm{Re}(\alpha_{\nu'}),$$

where

$$c_{\nu,\nu'} = \sum_x \Delta x\, f_\nu^+(x) f_{\nu'}^-(x). \tag{27}$$

Averaging the square of the above over realizations we obtain

$$\langle A_\nu^2\rangle = \sum_{\nu'} c_{\nu\nu'}^2\langle \mathrm{Re}^2(\alpha'_\nu)\rangle = \sum_{\nu'} c_{\nu\nu'}^2\frac{k_B T}{2\hbar\omega_{\nu'}},$$

where we used

$$\langle \mathrm{Re}(\alpha_\nu)\mathrm{Re}(\alpha_{\nu'})\rangle = \delta_{\nu\nu'}\frac{k_B T}{2\hbar\omega_\nu},$$

implied by the probability distribution (15). The above equations let us calculate two quantities $\langle A_\nu^2\rangle$ and

$$B_\nu = \sum_{\nu'} c_{\nu\nu'}^2\frac{k_B}{2\hbar\omega_{\nu'}}.$$

In Fig. 3 we plot B_ν. For modes between 600 and 800 the values of B_ν oscillate between zero and unity, and for modes above 800 the function B_ν is almost zero. The observed very small values of B_ν are caused by the fact that for certain ν, the function f_ν^+ vanishes in the bulk region of the quasicondensate and is located in the thermal cloud. In Fig. 4 we plot the values of $T_\nu/T_{\rm in}$, where $T_\nu = \langle A_\nu^2\rangle/B_\nu$ for those ν for which B_ν takes nonzero values. Additionally, we plot $T_\nu/T_{\rm in}$ obtained in the same way but for an initial state for which we set the value of $\psi(x,0) = 0$ for $|x| \geqslant x_0$. Two plots correspond to $T_{\rm in} = 50$ and 200 nK. We observe that $T_\nu/T_{\rm in}$ is close unity for both temperatures, when we took ψ being nonzero in the whole system, while $T_\nu/T_{\rm in}$ is about 0.6

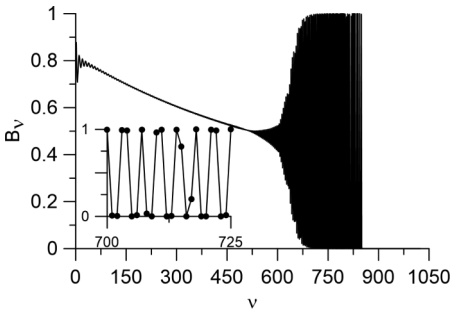

FIG. 3. The function B_ν. In the inset we plot the magnification in the smaller range to show the rapid oscillation.

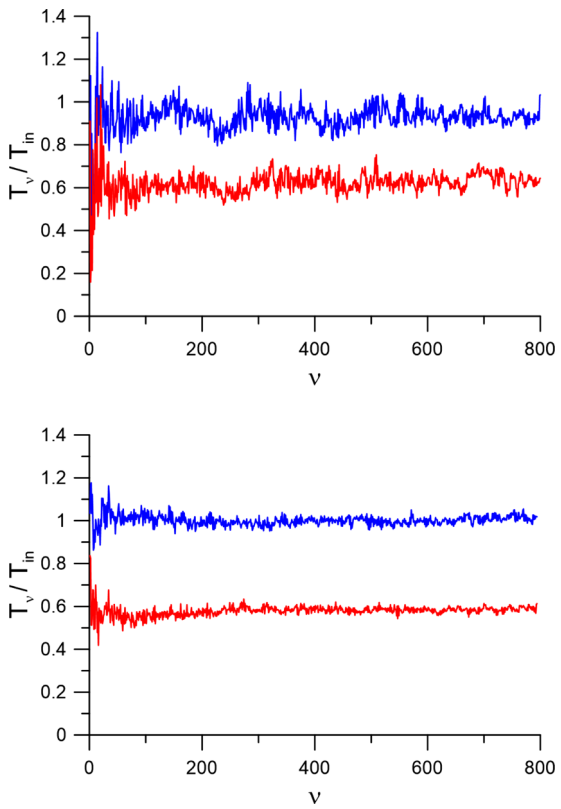

FIG. 4. Fraction $T_\nu/T_{\rm in}$ for $T_{\rm in} = 50$ nK (upper) and $T_{\rm in} = 200$ nK (lower). The lower curve corresponds to the case when the initial field was zero outside the region $|x| > x_0$, whereas the upper one is given for the initial field being nonzero everywhere. We observe that the upper curve oscillates around unity whereas the lower one is around 0.6.

for ψ being zero at the borders of the system. We draw the following conclusions from the results presented in the figure. First, the presented results show the necessity of a correct introduction of the classical field outside the bulk region. For small temperatures a fraction of the norm of ψ located in that region is very small and it is tempting to neglect it. Still, in this small fraction a lot of the energy of the system is stored and that is why it cannot be neglected. Second, the fact $T_v \simeq T_{\text{in}}$ implies that the temperature of the thermalized state is T_{in} with a relatively small error. The third conclusion is connected with the choice of the field $\psi(x, 0)$ outside the bulk region. It is rather obvious that the thermalized field differs from our choice. However, the initial field serves only as a state that needs to be thermalized and any way of constructing the tails of the field is correct as long as $T_v \simeq T_{\text{in}}$. The fact that this condition is satisfied in the discussed examples justifies our choice of the field.

As it can be seen from Eq. (26), we diagnosed the temperature using only density fluctuations but not phase fluctuations. The reason is that the contribution of each of the modes to the density fluctuation does not depend crucially on the mode while in the phase fluctuations only low modes contribute. This makes it almost impossible to extract a high mode contribution, making it useless for temperature diagnostics.

IV. ATOMIC PAIR CREATION PROCESS

After discussing the way of preparing the initial state we move to the atomic pair creation process. In the experiment [6] the time variation of the effective one-dimensional interaction parameter is obtained via a change of the trap frequencies, which is due to the temporal change of the laser intensity. In the experiment the trap frequency oscillation is given by

$$\omega_{x,r}(t) = \omega_{x,r}(1 + h\cos\omega_m t), \tag{28}$$

where $h = 0.05$ and $\omega_m = 2\pi \times 2170$ Hz. In Ref. [18] the authors analyze the dynamics of the three-dimensional (3D) cold gas. They find in a certain approximation that the density profile $n_{3d}(\mathbf{r}, t)$ keeps its initial shape with the change of the relative width $\lambda_{x,r}(t)$ i.e.,

$$n_{3d}(\mathbf{r}, t) \simeq \frac{1}{\lambda_x(t)\lambda_r^2(t)} n_{3d}\left(\frac{x}{\lambda_x(t)}, \frac{y}{\lambda_r(t)}, \frac{z}{\lambda_r(t)}\right),$$

where $n_{3d}(\mathbf{r})$ is the initial density profile given by the solution of Eq. (3). According to Ref. [18], the change of the width relative to the width $\lambda_{x,r}(t)$ is given by the equations

$$\ddot{\lambda}_r = \frac{\omega_r^2(0)}{\lambda_x\lambda_r^3} - \omega_r^2(t)\lambda_r, \tag{29}$$

$$\ddot{\lambda}_x = \frac{\omega_x^2(0)}{\lambda_x^2\lambda_r^2} - \omega_x^2(t)\lambda_x. \tag{30}$$

As $h \ll 1$, we approximate $\omega_{x,r}^2(t) \simeq \omega_{x,r}^2(0)(1 + 2h\cos\omega_m t)$. We substitute $\lambda_{x,r} = 1 + \delta\lambda_{x,r}$ and linearize the above equations with respect to $\lambda_{x,r}$. Then, the solution is

$$\delta\lambda_r \simeq \frac{h\omega_r}{(2\omega_r)^2 - \omega_m^2}[\omega_m \sin(2\omega_r t) - 2\omega_r \sin(\omega_m t)]. \tag{31}$$

The amplitude of $\delta\lambda_x$ is by a factor $\omega_x^2/\omega_r^2 \ll 1$ smaller than the amplitude $\delta\lambda_r$ and therefore can be neglected. The relative change of the radial width leads to the temporal change of $g(x)$ given by the expression

$$g(x, t) \simeq \frac{g(x)}{\lambda_r^2(t)} \simeq g(x)[1 - 2\delta\lambda_r(t)]. \tag{32}$$

We see that $g(x, t)$ oscillates with two different frequencies ω_m and $2\omega_r$, which are close to each other.

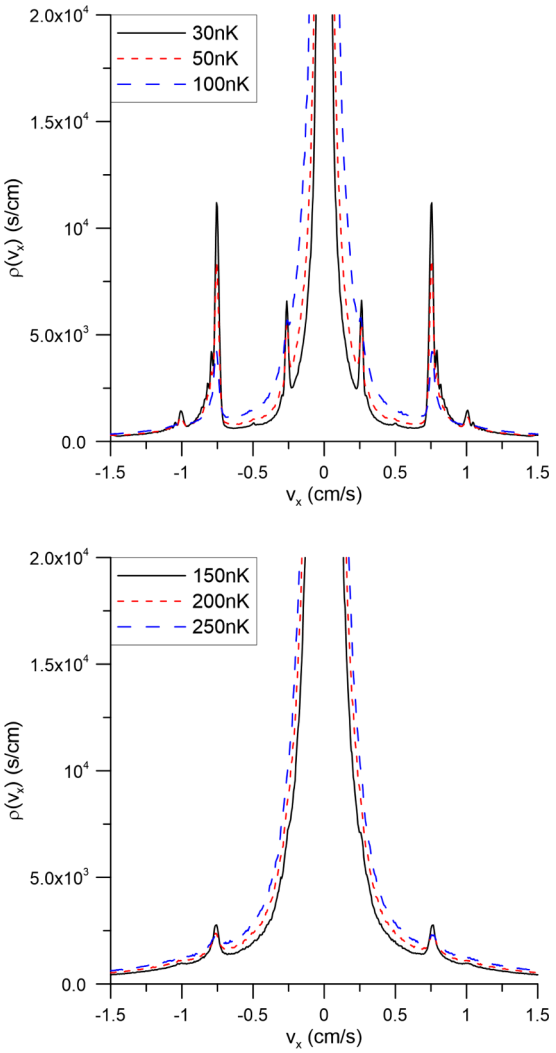

FIG. 5. Momentum density $\rho(v_x) = \frac{1}{N_r}\sum_{r=1}^{N_r} |\psi_r(v_x, t_f)|^2$ averaged over $N_r = 5000$ realizations.

A. Inhomogeneous system

Now we proceed with numerical simulations towards the true experimental situation. We take the initial state as the final state obtained in the previous section and evolve it for $t_f = 25$ ms using the GP equation (7) with $g(x, t)$ given by Eqs. (31) and (32).We repeat the procedure many times to obtain the average over realizations. In Fig. 5 we plot the momentum density of the classical field $\rho(v_x) = \frac{1}{N_r}\sum_{r=1}^{N_r} |\psi_r(v_x, t_f)|^2$ averaged over $N_r = 5000$ realizations for a few initial temperatures. The field is normalized $\sum_{v_x} \Delta v|\psi(v_x, t_f)|^2 = N$ with $\Delta v = \frac{2\pi\hbar}{mL}$. We notice a huge central peak which is given by the quasicondensate

distribution whose width grows with temperature, as expected. In the tails of the distribution we notice pairs of peaks. For low temperatures (first panel) we notice three pairs of peaks with velocities $|v_x| \simeq 0.25$, 0.8, and 1 cm/s. Using the homogeneous case calculation presented in the following section we find that the peaks with velocities 0.8 and 1.0 cm/s correspond to frequencies ω_m and $2\omega_r$, respectively. The third peak with a velocity 0.25 cm/s corresponds roughly to a frequency $2\omega_r - \omega_m$, which is a clear sign of frequency mixing taking place in the system. The highs of all the peaks produced by the temporal modulation of the interaction parameter decrease with increasing temperature so that at higher temperatures (second panel) only the ω_m peaks are visible.

In the experiment the system is suddenly released from the trap at time t_f. We simulate this part of the experiment to check if expansion changes the momentum density. To model the ballistic expansion we solve Eq. (29), obtaining in that case $\lambda_r(t) = \sqrt{1+\omega_r^2 t^2}$. It gives us an effective change of the one-dimensional interaction parameter $g(x,t) = g(x)/(1+\omega_r^2 t^2)$. With such an interaction parameter and taking $V(x) = 0$ to model the expansion, we further evolved the GP equation (7) for time $t_0 \simeq 30/\omega_r$. After that time $g(t)$ is so small that it can be practically neglected. Then, the evolution is linear with an unchanged momentum distribution. We calculated the final momentum density and compared it with the one before the release of the trap (at the end of modulation period). We have not found any noticeable differences.

Let us now compare the momentum density for $T = 200$ nK (which is the temperature in the experiment [6]) plotted in Fig. 5 with the one measured in the experiment that can be seen in Fig. 1(e) of Ref. [6]. We notice that the position of the peaks in the experiment resembles the one coming from numerical simulations. The same applies to the amplitude of the peak with respect to the background given by the tails of the central peak. Thus we notice a good agreement between the theoretical calculation and the experimental results.

In Ref. [6] the authors also compared the intensity differences in the two peaks. One of the possibilities to do this is to calculate the so-called number squeezing parameter defined as

$$s(t) = \frac{\langle[\hat{N}_+(t) - \hat{N}_-(t)]^2\rangle - \langle[\hat{N}_+(t) - \hat{N}_-(t)]\rangle^2}{\langle[\hat{N}_+(t) + \hat{N}_-(t)]\rangle}, \quad (33)$$

where

$$\hat{N}_\pm(t) = \sum_{|k \mp k_0| < \Delta k_0} \Delta k\, \hat{\Psi}^\dagger(k,t)\hat{\Psi}(k,t) \quad (34)$$

is the operator describing the number of particles in the peak whose maximum is located at $\pm k_0$. The condition $s < 1$, together with $\langle \hat{N}_+ \rangle = \langle \hat{N}_- \rangle$, implies the particle entanglement of the quantum state [12]. In the classical field method the above takes the form

$$N_\pm(t_f) = \sum_{|v \mp v_0| < \Delta v_0} \Delta v\, |\psi(v_x, t_f)|^2$$

and

$$s(t) = \frac{\langle[N_+(t) - N_-(t)]^2\rangle - \langle[N_+(t) - N_-(t)]\rangle^2}{\langle[N_+(t) + N_-(t)]\rangle}, \quad (35)$$

where $\Delta v = \frac{2\pi\hbar}{mL}$ and $\psi(v_x, t_f)$ is the classical field in a single realization at final time t_f. Using the above formulas we calculated numerically $s(t_f)$ for an experimental temperature $T = 200$ nK and for a few values of Δv_0. We found the minimal value of $s(t_f)$ being close to 9. This is in agreement with experimental measurements as the authors of Ref. [6] report the lack of sub-Poissonian fluctuations [19].

Finally, we comment on the number squeezing calculation in the classical field method. Here, we face the problem of operator ordering. We note that in the formula for the number squeezing parameter the numerator is quadratic in the number operator. Thus the difference coming from the different ordering of the operators in the numerator is roughly equal to the number operator which is present in the denominator of the number squeezing formula. This shows that different choices of the operator ordering result in the difference in the number squeezing parameter of the order of unity. Thus the uncertainty of the s parameter calculation given by the classical field method can be estimated to be equal to one. So in fact the result in the inhomogeneous case is $s \simeq 9 \pm 1$, which still gives a lack of sub-Poissonian fluctuations in the system.

We briefly summarize that the classical field simulation results are in agreement with the experimental measurements. However, to understand the theoretical results, we move to the homogeneous case analysis.

B. Homogeneous case

To simplify the analysis we take

$$\begin{aligned} g(t) &= g(0)\left(1 + 2\frac{h\omega_r}{(2\omega_r)^2 - \omega_m^2} 2\omega_r \sin(\omega_m t)\right) \\ &= g(1 + \epsilon \sin\omega_m t), \end{aligned} \quad (36)$$

which is equal to $g(x = 0, t)$ given by (32) with $\sin(2\omega_r t)$ neglected. As before, we chose the density to be given by the maximal density of the homogeneous case.

1. Bogoliubov method

First, we perform a Bogoliubov analysis of the pair production process similar to that in Ref. [13]. In such a case we do not use the classical field approximation but stay with a quantum field theory analysis. In the Bogoliubov method we use the density and phase operator representation of the field operator [17]

$$\hat{\Psi} = e^{i(\phi + \hat{\phi})}\sqrt{n + \delta\hat{n}},$$

together with the mode decomposition

$$\delta\hat{n}(x,t) = \sqrt{n}\sum_k f_k^-(x)\hat{a}_k(t) + \text{H.c.},$$

$$\delta\hat{\phi}(x,t) = \frac{1}{2\sqrt{n}}\sum_k -i f_k^+(x)\hat{a}_k(t) + \text{H.c.}$$

The equation of motion for the density $\delta\hat{n}$, phase ϕ, and phase operator $\hat{\phi}$ reads [17]

$$-\hbar\frac{\partial\phi}{\partial t} = g(t)n,$$
$$\hbar(\partial\delta\hat{n}/\sqrt{n})/\partial t = -\frac{\hbar^2}{2m}\frac{\partial^2}{\partial x^2}(2\hat{\phi}\sqrt{n}),$$
$$-\hbar\frac{\partial(2\sqrt{n}\hat{\phi})}{\partial t} = \left(-\frac{\hbar^2}{2m}\frac{\partial^2}{\partial x^2} + 2g(t)n\right)\frac{\delta\hat{n}}{\sqrt{n}}.$$

Inserting the mode decomposition into the above, we find

$$\frac{d}{dt}\hat{a}_k = -i\omega_k\left(\frac{E_k + [g(t)+g]n}{E_k + 2gn}\hat{a}_k + \frac{[g(t)-g]n}{E_k+2gn}\hat{a}^\dagger_{-k}\right).$$

Here, the functions $f_k^\pm$ are given by Eq. (16). We now take $g(t) = g(1+\epsilon\sin\omega_m t)$ given by Eq. (36) where $\epsilon \ll 1$ and approximate $\frac{E_k+[g(t)+g]n}{E_k+2gn} \simeq 1$. We additionally assume that $|\omega_m - 2\omega_k| \ll \omega_m$ which enables us to use the rotating-wave approximation so that the above equation takes the form

$$i\frac{d}{dt}\hat{a}_k = \omega_k\left(\hat{a}_k + i\frac{\epsilon gn}{2(E_k+2gn)}e^{-i\omega_m t}\hat{a}^\dagger_{-k}\right),$$

with the solution

$$\hat{a}_k(t) = \left(\cosh\Omega_k t + i\frac{\Delta_k}{\Omega_k}\sinh\Omega_k t\right)e^{-i\omega_m t/2}\hat{a}_k(0) + \frac{\delta_k}{\Omega_k}\sinh\Omega_k t e^{-i\omega_m t/2}\hat{a}^\dagger_{-k}(0), \quad (37)$$

where

$$\delta_k = \omega_k\frac{\epsilon gn}{2(E_k+2gn)},$$
$$\Delta_k = \omega_m/2 - \omega_k, \quad \Omega_k = \sqrt{\delta_k^2 - \Delta_k^2}.$$

We find the resonance at k_0 satisfying $\omega_m = 2\omega_{k_0}$ with the resonance width approximately equal to δ_{k_0}.

The above describes the quasiparticle properties. We now turn our attention to the particle properties. In Appendix A we establish an approximate connection between the quasiparticle and particle properties of the system. We find that the particle momentum density is approximately equal to

$$\langle\hat{\Psi}^\dagger(k,t)\hat{\Psi}(k,t)\rangle = N\rho(k) + \rho(k-k_0)\langle\hat{b}^\dagger_{k_0}(t)\hat{b}_{k_0}(t)\rangle + \rho(k+k_0)\langle\hat{b}^\dagger_{-k_0}(t)\hat{b}_{-k_0}(t)\rangle, \quad (38)$$

where

$$\hat{b}_k(t) = u_k\hat{a}_k(t) - v_k\hat{a}^\dagger_{-k}(t) \quad (39)$$

and

$$\sum_k \Delta k\,\rho(k) = 1,$$

with $\Delta k = \frac{2\pi}{L}$. By inspecting Eq. (38) we find that the particle momentum distribution has three peaks. The central one, equal to $N\rho(k)$, represents the quasicondensate momentum distribution. The two other peaks represent the resonant quasiparticle modes centered around $k = \pm k_0$. We notice that the shape of the peaks is given by the quasicondensate momentum distribution. Substituting experimental values we find $\hbar k_0/m \simeq 0.8$ cm/s, which is the same as the value of the center of the peaks in the momentum distribution observed experimentally.

In the experiment [6] the authors measured the properties of the number of particles in both peaks. Above we introduced operator $\hat{N}_\pm$ defined by Eq. (34) describing the number of particles in the peak located at $\pm k_0$. Assuming that Δk_0 present in the definition of $\hat{N}_\pm$ is such that it covers most of the peak, we show in Appendix A that

$$\hat{N}_\pm(t) \simeq \hat{b}^\dagger_{\pm k_0}(t)\hat{b}_{\pm k_0}(t). \quad (40)$$

Applying the Bogoliubov results given by Eq. (37) and using Eq. (39) we find

$$\langle\hat{N}_\pm(t)\rangle \simeq \langle\hat{b}^\dagger_{\pm k_0}(t)\hat{b}_{\pm k_0}(t)\rangle = u^2_{k_0}n_{k_0}(t) + v^2_{k_0}[n_{k_0}(t)+1], \quad (41)$$

where

$$n_{k_0}(t) = \langle\hat{a}^\dagger_{k_0}(t)\hat{a}_{k_0}(t)\rangle = n_{k_0}\cosh^2\delta_{k_0}t + (n_{k_0}+1)\sinh^2\delta_{k_0}t, \quad (42)$$

and we took the initial state as a thermal one with

$$n_k = \langle\hat{a}^\dagger_k(0)\hat{a}_k(0)\rangle = [\exp(\hbar\omega_k/k_BT) - 1]^{-1}. \quad (43)$$

Taking the experimental parameters we find $\delta_{k_0} \simeq 170$ Hz, $v^2_{k_0} = u^2_{k_0} - 1 \simeq 0.55$, and $n_{k_0} \simeq 3.36$ for $T = 200$ nK and $t = t_f = 25$ ms. For such values we find $\langle N_\pm(t_f)\rangle \simeq 2\times10^4$, which is much larger than the value measured in the experiment. We also calculate the number squeezing parameter defined by Eq. (33). From Eqs. (39) and (40) we find

$$(\hat{N}_+ - \hat{N}_-)(t) = \left(\hat{a}^\dagger_{k_0}\hat{a}_{k_0} - \hat{a}^\dagger_{-k_0}\hat{a}_{-k_0}\right)(t), \quad (44)$$

where we used the normalization condition $u_k^2 - v_k^2 = 1$. Moreover, from Eq. (37) we find that

$$(\hat{a}^\dagger_k\hat{a}_k - \hat{a}^\dagger_{-k}\hat{a}_{-k})(t) = (\hat{a}^\dagger_k\hat{a}_k - \hat{a}^\dagger_{-k}\hat{a}_{-k})(0).$$

As a result, the numerator of the formula for the squeezing parameter is constant in time and is equal to

$$\langle[\hat{N}_+(t) - \hat{N}_-(t)]^2\rangle - \langle[\hat{N}_+(t) - \hat{N}_-(t)]\rangle^2 = 2n_{k_0}(n_{k_0}+1).$$

The denominator of the mentioned formula is equal to $\langle(\hat{N}_+(t) + \hat{N}_-(t))\rangle$ and according to Eqs. (41) and (42) grows in time. For the experimental parameters we find that $s(t_f) \simeq 7\times10^{-4}$, which is much smaller than unity, shows disagreement with experimental results where $s(t_f)$ is above unity.

As we see, the above calculations of the peak population properties show huge discrepancies with experimental measurements. This shows the necessity of taking into account the interaction between quasiparticles neglected in the Bogoliubov method. To take them into account we move to the classical field method.

2. *Classical field analysis*

The method is defined as follows. We take the initial state $\psi(x,0)$ as the thermal state obtained in the previous section. Then, we evolve the GP equation (7) for $t_f = 25$ ms as in the experiment taking $V(x) = 0$ and $g(x,t) = g(t)$ given by Eq. (36). We repeat the procedure many times to obtain the average over realizations. First, we calculate

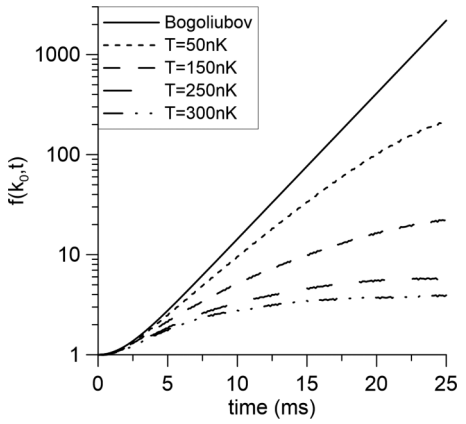

FIG. 6. The quasiparticle relative mode occupation $f(k_0, t) = \langle|\alpha_{k_0}(t)|^2\rangle/\langle|\alpha_{k_0}(0)|^2\rangle$ for the mode in resonance as a function of time for a few temperatures.

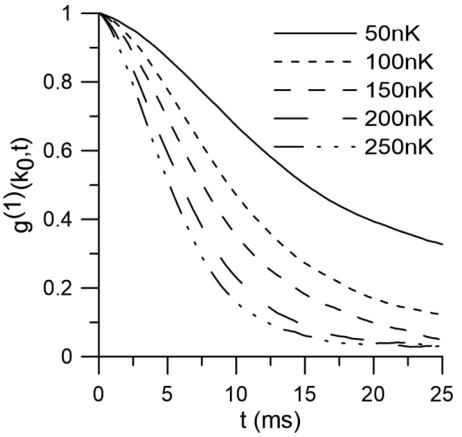

FIG. 7. The normalized single-particle correlation function $g_k(t)$ for the resonance mode as a function of time for a few temperatures.

$f(k_0, t) = \langle|\alpha_{k_0}(t)|^2\rangle/\langle|\alpha_{k_0}(0)|^2\rangle$, where the quasiparticle amplitude $\alpha_{k_0}(t)$ is given by Eq. (20). In Fig. 6 we plot this quantity for various temperatures. For comparison we draw the Bogoliubov prediction in the classical field method derived in Appendix B,

$$f(k_0, t) = \frac{\langle|\alpha_{k_0}(t)|^2\rangle}{\langle|\alpha_{k_0}(0)|^2\rangle} = \cosh\left(2\delta_{k_0}t\right).$$

We notice a dramatic drop in the production of quasiparticles with an increase in the temperature. For low temperatures the production tends to the Bogoliubov result. We also note that for smaller temperatures the quasiparticles are constantly produced in time, whereas for higher temperatures the number of quasiparticles produced tends to a constant, practically stopping after some critical time.

We interpret these facts in the spirit of Refs. [13,20]. In Ref. [13] a three-dimensional analog of the system considered here was discussed. There, the interaction between quasiparticles was taken into account in the description of the parametric amplification process. In the approximation assuming a lack of memory of self-energy functions, the interaction between quasiparticles enters the process only through the single parameter γ_k, which is simply the inverse of the quasiparticle lifetime. It was found that the pair production process practically stops in time when γ_{k_0} gets larger than the amplification parameter δ_{k_0} defined in the same way as in the Bogoliubov method described above. An interesting way of describing systems similar to the one considered was presented in Ref. [20]. There, the authors consider the Bogoliubov model as presented above. However, the interaction between quasiparticles is substituted by an interaction of quasiparticles with a large reservoir. The authors assume that the response of the reservoir to external perturbation is instantaneous in time (which is equivalent to the above-mentioned assumption of a lack of memory of the self-energy functions used in Ref. [13]). Then, it is not surprising that the interaction with the reservoir is effectively described by γ_k and that the results of Ref. [20] are the same as the one obtained in Ref. [13]. Still, the description presented in Ref. [20] that is quite general enables us to use the results obtained in Refs. [13,20] for the one-dimensional system considered here. They could be used in a straightforward way if the assumption of a lack of memory is satisfied. This can be verified by looking at the quasiparticle decay curve which is then exponential. Unfortunately, as we shall see below, this is not the case in our system. However, in the model considered in Ref. [20] or alternatively in the models of two modes coupled to a reservoir widely used in quantum optics [21], the quasiparticle decay curve can take different shapes depending on the reservoir memory functions used. Thus we expect that the condition $\delta_{k_0} \simeq \gamma_{k_0}$ for stopping the pair production process still applies to our system with γ_{k_0} describing the width of the quasiparticle decay curve.

Below, we check if the condition described above applies to our system. We calculate numerically the normalized single-particle correlation function

$$g^{(1)}(k_0, t) = \frac{\left|\langle\alpha^*_{k_0}(0)\alpha_{k_0}(t)\rangle\right|}{\langle|\alpha_{k_0}(0)|^2\rangle}$$

for the resonant mode. The results of the numerical calculation are presented in Fig. 7. Looking at this figure, we clearly see that the curves are not exponential. Still, the half width decreases with increasing temperature, as expected. Looking at Fig. 6, we find that the quasiparticle production process practically stops for a temperature around 150 nK. For that temperature we find $\gamma_{k_0} \simeq 100$ Hz which is close to $\delta_{k_0} = 170$ Hz calculated above. It shows that the derived condition applies.

Additionally, we calculate the squeezing parameter. In order to do it we rewrite Eqs. (39) and (41) substituting $\hat{b}_k \to \beta_k$. We obtain

$$\beta_k(t) = u_k\alpha_k(t) - v_k\alpha^*_{-k}(t) \tag{45}$$

and

$$N_\pm(t) = \left|\beta_{\pm k_0}(t)\right|^2. \tag{46}$$

Using Eqs. (45) and (46) where $\alpha_k(t)$ is given by Eq. (20), we calculate all the observables needed in the calculation of the squeezing parameter given by Eq. (35). For the temperature

$T = 200$ nK we find $s(t_f) \simeq 3.3$. This is larger than unity but smaller than the value obtained in the inhomogeneous system case, which is close to 9. We think that the reason for the observed difference is the following. Looking at the velocity distribution shown at Fig. 5, we notice that for a temperature 200 nK the peak height compared to background density coming from the quasicondensate distribution is smaller than unity. It means that more than half of the particles contributing to the number of particles in the peak come from a thermal distribution. These particles are not correlated in velocities and rather contribute to the increase of the number squeezing parameter. On the other hand, the value in the homogeneous case is obtained assuming a lack of quasicondensate particles in the side peaks. That is probably why the value of $s(t_f)$ calculated in the homogeneous case is smaller than in the nonhomogeneous case. However, it is important to notice that both values give a lack of sub-Poissonian fluctuations in the system.

V. SUMMARY

In the present paper we performed numerical simulations of an experiment [6] using the classical field method. The atomic pairs were created using a temporal modification of the effective interaction parameter. The results found are in full agreement with the experimental measurements. To understand the theoretical results we additionally analyzed the homogeneous analog of the experimental system. Analytical calculations within the Bogoliubov method were performed together with numerical simulations using the classical field approximation. The results of the Bogoliubov method show a pair production that is much larger than observed experimentally. The classical field analysis showed agreement with Bogoliubov results for temperatures significantly smaller than in the experiment. For higher temperatures it predicted a dramatic decrease of the number of pairs produced, in agreement with the experiment. We additionally calculated the number squeezing parameter for both homogeneous and inhomogeneous systems. We found that number squeezing does not take place, which is in agreement with experimental measurements. We interpreted these results in the spirit of the findings presented in Refs. [13,20]. There it was shown that the interaction between quasiparticles omitted in the Bogoliubov method (and accounted for in the classical field approximation) may dramatically influence the pair production process as well as the value of the number squeezing parameter. It was shown that the pair production process practically stops when the parameter δ_{k_0} describing the enhancement of the resonant mode, derived within the Bogoliubov method, is roughly equal to the quasiparticle decay constant γ_{k_0} which appears as a consequence of the interaction between quasiparticles. We numerically calculated γ_{k_0} and the atomic pair production as a function of temperature together with the δ_{k_0} parameter. We have shown that indeed the pair production process gets frozen when $\gamma_{k_0} \simeq \delta_{k_0}$. Additionally, we have shown that the experiment is in the regime when the pair production process gets frozen after a short time. This explains the fact of a relatively small number of generated atomic pairs observed in the experiment.

ACKNOWLEDGMENTS

We acknowledge discussions with Chris Westbrook, Denis Boiron, and Dimitri Gangardt.

APPENDIX A: CONNECTION BETWEEN QUASIPARTICLE AND PARTICLE PROPERTIES FOR HOMOGENEOUS SYSTEM

In this Appendix we establish an approximate relation between the quasiparticle and particle properties of the homogeneous system. We have

$$\hat{\Psi} = e^{i(\phi+\hat{\phi})}\sqrt{n+\delta\hat{n}},$$

together with the mode decomposition

$$\delta\hat{n}(x,t) = \sqrt{n}\sum_k f_k^-(x)\hat{a}_k(t) + \text{H.c.},$$

$$\delta\hat{\phi}(x,t) = \frac{1}{2\sqrt{n}}\sum_k -if_k^+(x)\hat{a}_k(t) + \text{H.c.},$$

where $f_k^\pm$ are given by Eq. (16). The modes of the system can be divided into low- and high-energy ones. Low-energy modes are highly populated and responsible for phase fluctuations of the system. The population of high-energy modes in the equilibrium state is much smaller than the population of low-lying modes. We divide $\hat{\phi} = \hat{\phi}_l + \hat{\phi}_h$, $\delta\hat{n} = \delta n_l + \delta n_h$, and approximate

$$\hat{\Psi}(x) = e^{i(\phi+\hat{\phi})}\sqrt{n+\delta\hat{n}} \simeq e^{i(\phi+\hat{\phi}_l)}\sqrt{n}\left(1 - i\hat{\phi}_h + \frac{\delta\hat{n}_h}{2n}\right).$$

Inserting into the above the mode decomposition, one obtains

$$\hat{\Psi}(x) \simeq \frac{1}{\sqrt{L}}e^{i(\phi+\hat{\phi}_l)}\left[\sqrt{N} + \sum_{k\in h}(u_k e^{ikx}\hat{a}_k - v_k e^{-ikx}\hat{a}_k^\dagger)\right],$$

where we used $f_k^\pm = u_k \pm v_k$. We further simplify the above by treating the phase operator of the low-energy modes (which are all highly populated) classically, $\hat{\phi}_l \to \phi_l$. Having done that we introduce the classical field of the low-energy modes defined as

$$\psi_c(x,t) = \frac{1}{\sqrt{L}}e^{i[\phi(t)+\phi_l(x,t)]}. \tag{A1}$$

Using that field and additionally introducing

$$\hat{b}_k(t) = u_k\hat{a}_k(t) - v_k\hat{a}_{-k}^\dagger(t),$$

we arrive at

$$\hat{\Psi}(x,t) \simeq \psi_c(x,t)\left(\sqrt{N} + \sum_{k\in h} e^{ikx}\hat{b}_k(t)\right).$$

Inserting the above into

$$\hat{\Psi}(k,t) = \frac{1}{\sqrt{2\pi}}\sum_j \Delta x\, e^{-ikx}\hat{\Psi}(x,t),$$

we arrive at

$$\hat{\Psi}(k,t) \simeq \sqrt{N}\psi_c(k,t) + \sum_p \psi_c(k-p,t)\hat{b}_p(t), \tag{A2}$$

where

$$\psi_c(k,t) = \frac{1}{\sqrt{2\pi}} \sum_x \Delta x\, e^{-ikx} \psi_c(x,t). \tag{A3}$$

We assume that the influence of the high-energy sector on the dynamics of the low-energy sector can be neglected. Thus the classical phase $\phi(t) + \phi_l(x,t)$ describes the evolution of the thermal state. This implies that the averages of the field $\psi_c(x,t)$ are the thermal state averages that do not depend on time.

We further assume that among all high-energy modes only two resonance modes with $k = \pm k_0$ have a significant population. Thus we have

$$\langle \hat{\Psi}^\dagger(k,t)\hat{\Psi}(k,t)\rangle = N\rho(k) + \rho(k-k_0)\langle \hat{b}^\dagger_{k_0}(t)\hat{b}_{k_0}(t)\rangle + \rho(k+k_0)\langle \hat{b}^\dagger_{-k_0}(t)\hat{b}_{-k_0}(t)\rangle, \tag{A4}$$

where

$$\rho(k) = \langle |\psi_c(k,t)|^2\rangle.$$

In the above formula we used the fact that the average $\langle |\psi_c(k,t)|^2\rangle$ does not depend on time. Using Eqs. (A1) and (A3) we find that ρ is normalized to unity, i.e.,

$$\sum_k \Delta k\, \rho(k) = 1,$$

where $\Delta k = \frac{2\pi}{L}$. We introduce the operators

$$\hat{N}_\pm = \sum_{|k\mp k_0|<\Delta k_0} \Delta k\, \hat{\Psi}^\dagger(k)\hat{\Psi}(k).$$

Using Eq. (A2) and the fact that $\psi_c^*(k)\psi_c(k \pm k_0) \simeq 0$, we find

$$\hat{N}_\pm = \sum_{|k\mp k_0|<\Delta k_0} \Delta k |\psi_c(k \mp k_0)|^2 \hat{b}^\dagger_{\pm k_0}\hat{b}_{\pm k_0}.$$

From Eqs. (A1) and (A3) we obtain

$$\sum_{|k\mp k_0|<\Delta k_0} \Delta k |\psi_c(k \mp k_0)|^2 \simeq 1.$$

To obtain the above we assumed that Δk_0 is such that it covers most of the peak. As a result, we find

$$\hat{N}_\pm \simeq \hat{b}^\dagger_{\pm k_0}\hat{b}_{\pm k_0}.$$

APPENDIX B: THE BOGOLIUBOV METHOD IN THE CLASSICAL FIELD APPROXIMATION

In this Appendix we use the results of the Bogoliubov method described in Sec. IV B 1 to find their analog in the classical field approximation. In the classical field method we substitute the annihilation and creation operators by c-numbers $\hat{a}_k \to \alpha_k$. Then the averages over $\alpha_k(0)$ are calculated using the probability distribution given by Eq. (15). For example,

$$\langle |\alpha_k(0)|^2\rangle = \frac{k_B T}{\hbar\omega_k}.$$

This corresponds to the quantum average

$$n_k = \langle \hat{a}^\dagger_k(0)\hat{a}_k(0)\rangle = [\exp(\hbar\omega_k/k_B T) - 1]^{-1}$$

in the limit $n_k \gg 1$. Applying the above procedure to Eq. (37) we find that

$$\langle |\alpha_k(t)|^2\rangle = \left(\sinh^2 \delta_{k_0} t + \cosh^2 \delta_{k_0} t\right)\langle |\alpha_k(0)|^2\rangle.$$

[1] L. Pezze, A. Smerzi, M. K. Oberthaler, R. Schmied, and P. Treutlein, arXiv:1609.01609.

[2] V. Giovannetti, S. Lloyd, and L. Maccone, Science **306**, 1330 (2004).

[3] O. Hosten, N. J. Engelsen, R. Krishnakumar, and M. A. Kasevich, Nature (London) **529**, 505 (2016).

[4] P. Bouyer and M. A. Kasevich, Phys. Rev. A **56**, R1083 (1997).

[5] J. A. Dunningham, K. Burnett, and S. M. Barnett, Phys. Rev. Lett. **89**, 150401 (2002).

[6] J. C. Jaskula, G. B. Partridge, M. Bonneau, R. Lopes, J. Ruaudel, D. Boiron, and C. I. Westbrook, Phys. Rev. Lett. **109**, 220401 (2012).

[7] M. Bonneau, J. Ruaudel, R. Lopes, J. C. Jaskula, A. Aspect, D. Boiron, and C. I. Westbrook, Phys. Rev. A **87**, 061603 (2013).

[8] R. Bücker, J. Grond, S. Manz, T. Berrada, T. Betz, C. Koller, U. Hohenester, T. Schumm, A. Perrin, and J. Schmiedmaye, Nat. Phys. **7**, 608 (2011).

[9] T. Wasak, P. Szań kowski, R. Bücker, J. Chwedeń czuk, and M. Trippenbach, New J. Phys. **16**, 013041 (2014).

[10] B. Wu and Q. Niu, Phys. Rev. A **64**, 061603 (2001).

[11] I. Carusotto, R. Balbinot, A. Fabbri, and A. Recati, Eur. Phys. J. D **56**, 391 (2010).

[12] T. Wasak, P. Szańkowski, P. Ziń, M. Trippenbach, and J. Chwedeńczuk, Phys. Rev. A **90**, 033616 (2014).

[13] P. Ziń and M. Pylak, J. Phys. B **50**, 085301 (2017).

[14] K. Góral, M. Gajda, and K. Rzążewski, Phys. Rev. A **66**, 051602 (2002).

[15] F. Gerbier, Europhys. Lett. **66**, 771 (2004).

[16] For the considered system we have $k_B T/(\hbar\omega_r) \simeq 2.8$. Thus the above assumption is, strictly speaking, not fulfilled. Still, the modes contribute as k^{-2} (for the uniform system) to the phase fluctuations which are responsible for the quasicondensate velocity profile. As shown below, this profile is the quantity that determines the properties of the atomic pairs created by parametric resonance. Therefore for our analysis the model is a good approximation of the true experimental situation.

[17] D. S. Petrov, D. M. Gangardt, and G. V. Shlyapnikov, J. Phys. IV France **116**, 5 (2004).

[18] Y. Castin and R. Dum, Phys. Rev. Lett. **77**, 5315 (1996).

[19] Sub-Poissonian fluctuation means $s < 1$.

[20] X. Busch, R. Parentani, and S. Robertson, Phys. Rev. A **89**, 063606 (2014).

[21] D. F. Walls and G. J. Milburn, *Quantum Optics*, 2nd ed. (Springer, Berlin, 2008).